PHYSICAL REVIEW D VOLUME 8, NUMBER 12 15 DECEMBER 1973

Quantum Electrodynamics and Renormalization Theory in the Infinite-Momentum Frame*

Stanley J. Brodsky
Stanford Linear Accelerator Center, Stanford, California 94305

Ralph Roskies†‡
Yale University, New Haven, Connecticut 06520

Roberto Suaya§
Stanford Linear Accelerator Center, Stanford, California 94305
(Received 30 July 1973)

Time-ordered perturbation theory evaluated in the infinite-momentum reference frame of Weinberg is shown to be a viable calculational alternative to the usual Feynman graph procedure for quantum electrodynamics. We derive the rules of calculation at infinite momentum, and introduce a convenient method for automatically including z graphs (backward-moving fermion contributions). We then develop techniques for implementing renormalization theory, and apply these to various examples. We show that the $P \to \infty$ limit is uniform for calculating renormalized amplitudes, but this is not true in evaluating the renormalization constants themselves. Our rules are then applied to calculate the electron anomalous moment through fourth order and a representative diagram in sixth order. It is shown that our techniques are competitive with the normal Feynman approach in practical calculations. Some implications of our results and connections with the light-cone quantization are discussed.

I. INTRODUCTION

Over the past few years it has been shown that the use of an "infinite-momentum" Lorentz frame[1] has remarkable advantages for calculations in elementary particle physics and field theory, especially in the areas of current-algebra sum rules,[2] parton models,[3,4] and eikonal scattering.[5,6] One important advantage is that it allows a straightforward application of the impulse and incoherence approximations familiar in nonrelativistic atomic and nuclear physics to relativistic field-theory and bound-state problems.

We shall show that infinite-momentum-frame methods are also competitive with the usual Feynman methods in quantum electrodynamics (QED). Despite the passage of over two decades, the basic methods for calculations in QED have changed little since the development of the Feynman-Dyson-Schwinger rules. Although it is true that dispersion-theory calculations of the lepton vertex—dispersing either in the photon mass or sidewise in one fermion leg—do provide such an alternative procedure, in fact such calculations are much more arduous than the standard Feynman method, often involving extremely subtle and treacherous nonuniform infrared problems,[7] and only are applicable to the two- and three-point amplitudes. The time-ordered perturbation-theory–infinite-momentum-frame method (TOPTh$_\infty$) to be described here retains the main advantages of the dispersion method since calculations involve physical on-mass-shell intermediate states of fixed particle number, but because of the $P \to \infty$ limit the complicated square-root structure of the phase-space integration is automatically linearized, and the analysis of infrared divergences is no more difficult than in the corresponding Feynman calculations.

The field-theoretic aspects of time-ordered perturbation theory in the $P \to \infty$ limit were first studied by Weinberg[1] in spinless theories. The development of the parton model[3] by Drell, Levy, and Yan motivated the extension of Weinberg's work to spin-$\frac{1}{2}$ theories.[4] Because of the equivalence of TOPTh$_\infty$ with conventional field theory demonstrated here for quantum electrodynamics (and by simple extension to the superrenormalizable ϕ^3 theory and the renormalizable $\bar{\psi}\gamma_5\psi\pi$ pseudoscalar theory), such parton-model calculations can acquire a rigorous basis. The important qualification is the necessity to use covariant regularization rather than a simple transverse-momentum-cutoff procedure in order to avoid difficulties with gauge invariance and covariance.

The $P \to \infty$ limit became of even greater interest when its relation to light-cone quantization was realized.[6] In fact, the standard rules of calculation are identical in the two theories. The z-graph contributions of the TOPTh$_\infty$ correspond to seagull terms in the interaction using the light-cone quantization method. However, the development of the calculational rules directly from the standard theory with the $P \to \infty$ limit allows one to develop renormalization theory and avoids errors due to nonuniform convergence in the $P \to \infty$ limit. For example, we clarify the subtleties involved in the light-cone calculation of the electron self-mass.

Our results agree with the analysis of this problem by Bouchiat *et al.*[8] Our techniques show how to calculate quantum electrodynamics on the light cone in the Feynman gauge, rather than in the Coulomb gauge, and how to implement the renormalization procedure.

After the work in this paper was completed, there have appeared other, more formal, proofs of the equivalence between light-cone and conventional QED.[9] The approaches are somewhat complementary. Whereas these works show formally that light-cone-formulated and conventional QED have the same renormalized S matrices, we show that the $P\to\infty$ limit of time-ordered perturbation theory does give the light-cone-formulated rules. Moreover, we use this formalism to perform actual higher-order calculations.

The plan of this paper is as follows: In Sec. II, we rederive the rules for calculating time-ordered perturbation theory (TOPTh) in the infinite-momentum frame, and present an automatic method for incorporating the contributing "z graphs" of spinor theories. Then, even in spinor theories only intermediate states in which each particle has a positive component of momentum along P survive in the $P\to\infty$ limit. Moreover, we show that a single spinor or trace calculation suffices for all time-ordered graphs corresponding to the same Feynman graph.

The renormalization procedure for TOPTh$_\infty$ is presented in Sec. III. We show that the $P\to\infty$ limit is uniformly convergent with respect to the phase-space integrations when calculating renormalized amplitudes with invariant regularization, although this is not true for the evaluation of the renormalization constants themselves. Vacuum polarization and the general problem of photon and fermion self-energy insertions in higher-order graphs are discussed. Examples of vertex subgraph renormalization in the fourth-order electron vertex are also discussed. This section also contains a proof of the Ward identity in the context of TOPTh$_\infty$, and a heuristic proof of the renormalizability of QED in TOPTh$_\infty$.

In Sec. IV we discuss some details of the calculation of the fourth-order and some pieces of the sixth-order anomalous magnetic moment of the electron. The required phase-space integrations over transverse and fractional longitudinal momenta are in general regular and smooth, and are often more readily integrable than the standard Feynman parametric form.

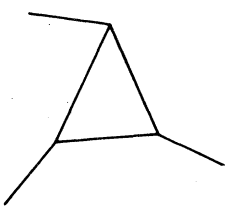

FIG. 1. Feynman vertex graph in third order.

In the Appendix we discuss a method which, in some cases, provides a direct connection between the Feynman rules and those at infinite momentum. This method provides further insight into how our z-graph rules arise. We also comment that the connection between the Feynman and TOPTh$_\infty$ rules is not simple in all cases.

II. THE RULES

The S matrix is related to the invariant matrix element M by

$$S=1-(2\pi)^4 i\,\delta^{(4)}(P_{\text{final}}-P_{\text{initial}})M\prod_{\substack{\text{external}\\ \text{particles}}}N_i, \tag{2.1}$$

where N_i is the normalization factor $(2\pi)^{-3/2}(2E_i)^{-1/2}$ and E_i is the energy of the ith external particle. We now write the rules for calculating the contributions to M in the interaction picture in TOPTh. For the moment we restrict ourselves to spinless particles with a ϕ^3 interaction. We first classify the time-ordered contributions according to their Feynman topologies. Then we do the following:

1. For each Feynman graph of order n, assign a time t_i to the ith vertex. Then draw $n!$ graphs, corresponding to all permutations of the times t_i, with the same topology as the Feynman graph. As an example, to the simple Feynman vertex graph of Fig. 1 there correspond six time-ordered graphs as shown in Fig. 2. (By convention, time flows from left to right.)

2. With each line of each time-ordered graph, associate a three-momentum.

3. At each vertex except the last, write a factor $(2\pi)^3 g\,\delta^{(3)}(\sum\vec{p}_i)$, where g is the coupling constant, and the δ function expresses three-momentum conservation at that vertex. At the last vertex insert only a factor g, since the factor $(2\pi)^3\delta^{(3)}(\sum\vec{p}_i)$ has already been taken out of M in (2.1).

4. For each internal line write a factor $(2\pi)^{-3}2E_i^{-1}$, where E_i is the energy of the line in question, calculated on the mass shell, i.e.,

$$E_i=(\vec{p}_i^{\,2}+m_i^2)^{1/2}. \tag{2.2}$$

5. For each intermediate state, i.e., for each state between interaction times, write a factor

$$\frac{1}{E_{\text{inc}}-E_{\text{int}}+i\epsilon},$$

where E_{inc} is the total energy of the incoming particles, and E_{int} is the energy of the intermediate

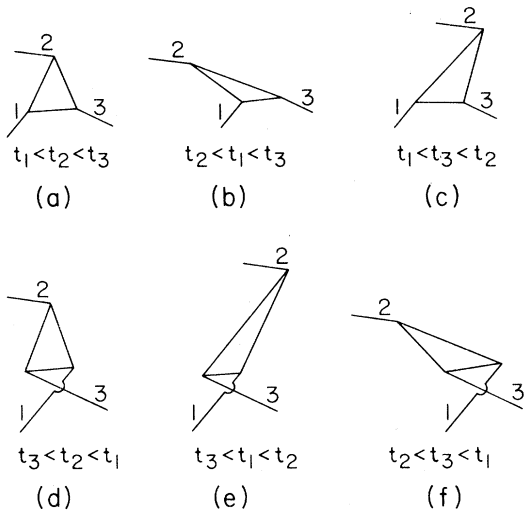

FIG. 2. The six time-ordered contributions to the Feynman vertex graph of Fig. 1. By convention, time flows from left to right.

state, obtained by adding the single-particle energies of all particles in that particular state.

6. Integrate d^3p_i.

7. Add the contributions of all the different time-ordered graphs.

One sees several features which distinguish TOPTh from the Feynman approach. First, every intermediate particle is on its mass shell, but energy is not conserved, while in the Feynman approach, energy is conserved but particles are off the mass shell. Second, all particles propagate forward in time, and the number of particles in a given intermediate state is clear. Third, manifest covariance is gone. One can summarize these last two points by saying that TOPTh emphasizes the unitarity of the theory, while the usual approach emphasizes its covariance. Fourth, there are many more graphs to calculate in TOPTh than in the Feynman approach.

Points three and four are usually considered serious practical shortcomings of TOPTh. However, Weinberg[1] realized that the lack of manifest covariance could be used to good advantage. He argued that since the sum of the time-ordered graphs was covariant, although each of the graphs by itself was not, it might be possible to find a frame of reference in which it was particularly simple to calculate each of these graphs. In particular, there might be a frame in which one could recognize immediately that most of the graphs gave a vanishing contribution. That frame is the infinite-momentum frame.

Let us review his argument. We view the scattering process from a frame moving rapidly in the negative z direction, so that the total incident momentum $\vec{P}$ is large and along the positive z direction. We will show that as $P\to\infty$, each of the time-ordered graphs tends to a finite limit, often to 0. That each graph tends to a finite limit is not a trivial result, since from covariance only the sum of all the graphs need be independent of P. There might have been cancellations between infinities of specific time-ordered graphs.

We parametrize the momentum of the ith line by

$$\vec{p}_i = x_i\vec{P} + \vec{k}_i , \tag{2.3}$$

where x_i is the fractional longitudinal momentum and $\vec{k}_i$ is a two-dimensional vector in the x-y plane.

Since by definition the total incident momentum is $\vec{P}$, we have

$$\sum_{\text{inc}} \vec{p}_i \equiv \left(\sum_{\text{inc}} x_i\right)\vec{P} + \sum_{\text{inc}} \vec{k}_i = \vec{P}$$

so that

$$\sum_{\text{inc}} x_i = 1 , \qquad \sum_{\text{inc}} \vec{k}_i = 0 . \tag{2.4}$$

Because of three-momentum conservation of each vertex, we also have for each intermediate state

$$\sum_{\text{int}} x_i = 1 , \qquad \sum_{\text{int}} \vec{k}_i = 0 . \tag{2.5}$$

Assuming that no photons are traveling exactly in the $-z$ direction, we can always choose the velocity of the observing frame large enough so that all external particles have their z component of momentum positive, i.e.,

$$x_i > 0 \tag{2.6}$$

for all external particles. But for internal particles, the x integrations extend over negative x as well.

In the limit $P\to\infty$, we have, from (2.2) and (2.3),

$$E_i = (\vec{p}_i^{\,2} + m_i^{\,2})^{1/2} = |x_i|P + \frac{s_i}{2P} + O\left(\frac{1}{P^3}\right) , \tag{2.7}$$

where

$$s_i = \frac{\vec{k}_i^{\,2} + m_i^{\,2}}{|x_i|} . \tag{2.8}$$

The incident energy is, by (2.6) and (2.4),

$$E_{\text{inc}} = \sum_{\text{inc}} E_i = P + \sum_{\text{inc}} \frac{s_i}{2P} + O\left(\frac{1}{P^3}\right) . \tag{2.9}$$

The energy of an intermediate state is

$$E_{\text{int}}=\sum_{\text{int}}\left(|x_i|P+\frac{s_i}{2P}\right)+O\left(\frac{1}{P^3}\right). \tag{2.10}$$

If all the x_i in the intermediate state are positive, then using (2.5) we find

$$E_{\text{int}}=P+\sum\frac{s_i}{2P}+O\left(\frac{1}{P^3}\right). \tag{2.11}$$

If, however, some x_i are negative, we have

$$E_{\text{int}}=\left(1-2\sum_{x_i<0}x_i\right)P+O\left(\frac{1}{P}\right). \tag{2.12}$$

Counting powers of P in a graph with n vertices, we obtain the following:

(a) From rule 3

$$\delta^{(3)}\left(\sum\vec{p}_i\right)=\delta^{(2)}(\sum\vec{k}_i)\delta((\sum x_i)P)$$

$$=\frac{1}{P}\delta^{(2)}(\sum\vec{k}_i)\delta(\sum x_i)$$

and since there are $(n-1)$ δ functions we obtain a factor $P^{-(n-1)}$.

(b) From rules 4 and 6

$$\frac{d^3p_i}{(2\pi)^3 2E_i}=\frac{d^2k dx}{2|x|(2\pi)^3}$$

independent of P.

(c) From rule 5 for each intermediate state with all $x_i>0$, we obtain from (2.9) and (2.11)

$$\frac{2P}{\sum_{\text{inc}}s_i-\sum_{\text{int}}s_i+i\epsilon},$$

whereas if some $x_i<0$, we obtain from (2.12)

$$\frac{1}{2\sum_{x_i<0}x_iP}.$$

s_i is given by (2.8). There are altogether $(n-1)$ intermediate states, and so to obtain a nonvanishing limit as $P\to\infty$, each term from rule 5 must contribute a factor P. Thus in all cases we have a finite limit and a nonzero limit only if each intermediate state has all its $x_i>0$. But since $\sum x_i$ is conserved at each vertex, this is only possible if each vertex has at least one line coming from the past and one line proceeding to the future. Thus, of the six graphs of Fig. 2, only 2(a) and 2(b) have nonvanishing limits as $P\to\infty$. So the passage to infinite momentum has reduced the number of graphs to be calculated. It should be stressed that letting $P\to\infty$ is just a choice of reference frame, and no invariant quantity is getting large.

We have been rather cavalier in counting powers of P, for although P gets large, it is possible that xP is not large, and our expansion (2.7) in terms of P may not be valid. This is discussed in greater detail in Sec. III. Our analysis is correct for the calculation of renormalized quantities, but must be modified for calculating divergent quantities.

We can now rewrite the rules of calculation, denoting them by primes:

1′. For each Feynman graph of order n, draw all time-ordered graphs in which each vertex has at least one line from the past and one to the future.

2′. With each line associate an x and $\vec{k}$.

3′. At each vertex except the last write a factor $(2\pi)^3 g\,\delta(\sum x_i)\delta^{(2)}(\sum\vec{k}_i)$ inserting only g at the last vertex.

5′. For each intermediate state write a factor

$$\frac{2}{\sum_{\text{inc}}s_i-\sum_{\text{int}}s_i+i\epsilon}.$$

4′ and 6′. Integrate

$$\frac{d^2k_i dx_i\theta(x_i)}{(2\pi)^3 2x_i}.$$

7′. Sum over all time-ordered graphs.

The presence of spin complicates the situation. In the case of QED, the vertex becomes one of the following[10]:

$$\bar{u}(p)e\gamma^\mu u(p')\epsilon_\mu, \tag{A}$$

$$\bar{u}(p)e\gamma^\mu v(p')\epsilon_\mu, \tag{B}$$

$$-\bar{v}(p)e\gamma^\mu u(p')\epsilon_\mu, \tag{C}$$

$$-\bar{v}(p)e\gamma^\mu v(p')\epsilon_\mu, \tag{D}$$

instead of g ($e^2=4\pi\alpha$). Here p and p' are the momenta of the respective on-mass-shell fermions [i.e., $p_0=(\vec{p}^2+m^2)^{1/2}$], and ϵ_μ is the polarization vector of the photon.

The sum over intermediate states now also involves the sum over spin. We work in the Feynman (Gupta-Bleuler) gauge, where

$$\sum_\lambda\epsilon_\mu(k,\lambda)\epsilon_\nu(k,\lambda)=-g_{\mu\nu}.$$

Our previous counting powers of P is now upset, since the vertices can also contribute powers of P. A straightforward calculation[11] shows that as $P\to\infty$, one of the vertices (A)–(D) is of order P only if

(a) $\mu=0$ or 3 and $xx'>0$,
(b) $\mu=1$ or 2 and $xx'<0$, (2.13)

Otherwise, it is of order unity. Moreover, in case (a), the coefficient of P is the same whether $\mu=0$ or $\mu=3$. (Here x and x' are the x values associated with p and p'.)

We now show that the contribution to M is of order $P^{N_1+N_3}$, where N_i is the number of external photons of polarization i.

Assume first that all $x_i>0$, so that case (b) never arises. If a vertex is connected to an external photon, it contributes a factor P if and only if the polarization is 0 or 3. If the vertex is connected to an internal photon, because the coefficient of P is the same whether $\mu=0$ or $\mu=3$, and because $g_{00}=-g_{33}$ in the photon polarization sum, the terms of order P and P^2 from these two vertices cancel identically, and give an effective vertex of order unity. (The terms of order unity do not cancel, so that one cannot say that the $\mu=0$ piece cancels the $\mu=3$ piece. In fact, this scalar/longitudinal piece is responsible for the Coulomb force.)

Suppose now that some $x_i<0$. We saw that the matrix element is suppressed by $1/P^2$ for every intermediate state containing a particle with $x<0$. But such a particle can contribute a factor P^2 to the numerator (a factor P for each of its two vertices). Thus, a fermion of negative x can contribute to M in leading order but only if (a) it extends over one time interval only, so that it contributes to only one intermediate state, and (b) the fermions at each of its vertices have $x>0$. Since a photon of negative x contributes no powers of P to the numerator, it can contribute only if every intermediate state containing it also contains a fermion of negative x. This is only possible in the simplest self-energy diagram (see Fig. 3) which will be discussed in Sec. III. These rules for incorporating fermions of negative x were first derived by Drell, Levy, and Yan.[11]

Because fermions of negative x can contribute to leading order, our previous criterion of discarding graphs with fermions of negative x is no longer valid. But it can be salvaged by modifying the fermion spin sum as we now show.

The spin sum occurring in the matrix elements is

$$\sum_s u(p,s)\bar{u}(p,s)=(\not{p}+m),$$

$$(-)\sum_s v(p,s)\bar{v}(p,s)=(-\not{p}+m).$$

Suppose there is a graph $\tilde{G}$ with a positron of momentum $\hat{p}_\mu$ with negative $\hat{x}$ between vertices V_1 and V_2 with V_2 after V_1. The energy denominator associated with the intermediate state between

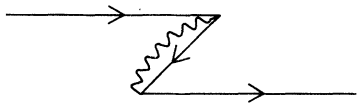

FIG. 3. Time-ordered contribution to the self-energy containing a backward-moving fermion.

V_1 and V_2 is $E_{\rm inc}-E_{\rm int}=2\hat{x}P$. (Note that no other particle occurring in this intermediate state can have negative x since it would extend over more than one time interval and give zero contributions. The exceptional cases are the self-energy graph of Fig. 3 and the corresponding photon self-energy graph with which we will deal separately.) It is straightforward to see that there is always an additional time-ordered graph G identical to $\tilde{G}$ except that the time order of vertices V_1 and V_2 is interchanged. The line between V_2 and V_1 now represents an electron with momentum $\vec{p}=-\hat{\vec{p}}$, $E_p=E_{\hat{p}}=(\vec{p}^2+m^2)^{1/2}$. The sum of contributions from these two intermediate states is

$$2P\frac{(\not{p}+m)}{s_{\rm inc}-s_{\rm int}+i\epsilon}+\frac{(-\not{\hat{p}}+m)}{2\hat{x}P}$$
$$=2P\left[\frac{(\not{p}+m)}{s_{\rm inc}-s_{\rm int}+i\epsilon}+\frac{-2E_p\gamma^0}{4\hat{x}P^2}+\frac{\not{p}+m}{4\hat{x}P^2}\right]. \quad (2.14)$$

The third term of (2.14) is negligible compared to the first. Also we have

$$E_p=|\hat{x}|P=-\hat{x}P \quad \text{since} \quad \hat{x}<0, \quad (2.15)$$

and so (2.14) becomes

$$2P\left[\frac{\gamma\cdot\tilde{p}+m}{s_{\rm inc}-s_{\rm int}+i\epsilon}+O\left(\frac{1}{P^2}\right)\right], \quad (2.16)$$

where

$$\tilde{p}_i=p_i, \quad i=1,2,3$$
$$\tilde{p}^0=p^0+\frac{s_{\rm inc}-s_{\rm int}}{2P}. \quad (2.17)$$

By changing the propagator of an electron with positive x from $(\not{p}+m)$ to $(\gamma\cdot\tilde{p}+m)$ whenever the electron line extends over a single time interval, we automatically take into account the contribution of all positrons with $x<0$. Similarly, we modify the propagator of positrons with positive x, which extends over one time interval, from $(-\gamma\cdot p+m)$ to $(-\gamma\cdot\tilde{p}+m)$. We do not change the propagators of fermion lines extending over more than one time interval. With the replacement (2.17) only time orders in which every intermediate state has positive-moving particles need to be explicitly considered.

This replacement of p_μ by $\tilde{p}_\mu$ is very reminiscent of the Feynman approach. One takes the fermion off the mass shell ($\tilde{p}^2 \neq m^2$), but reduces the number of diagrams. Moreover, $\tilde{p}_\mu$ is the four-vector which enforces four-momentum conversation between the given intermediate state and the *external* state:

$$(E_{\text{int}} - p_0) + \tilde{p}_0 = E_{\text{inc}} .$$

However, since not all fermion lines extend over a single time interval we do not have complete four-momentum conservation at every vertex.

From (2.13b) we see that it is not necessary to modify the propagator of a fermion extending over a single time interval if either of its vertices is connected to an external photon of polarization 0 or 3, although modifying it will not change the answer. This follows because the associated fermion of negative x cannot contribute the necessary P^2 to the numerator.

Our final rules for QED at infinite momentum are thus obtained by modifying the infinite-momentum rules for the ϕ^3 theory as follows:

2''. With each internal line associate an x and k. For $\binom{\text{electrons}}{\text{positrons}}$ extending over more than one time interval insert a factor $(\pm \not{p} + m)$, where p is the four-momentum associated with the line. For fermions extending over *one* time interval insert the factor $(\pm \gamma \cdot \tilde{p} + m)$, where $\tilde{p}$ is related to p by (2.17). For each internal photon line insert the factor $-g_{\mu\nu}$. A trace is implied for closed fermion loops.

3''. Replace g by $e\gamma^\mu$ in 3'.

Finally, we note that if we assign momenta $p_1, \ldots, p_N$ for the fermion momenta of a given graph, then the Dirac algebra for each time ordering is identical to that of the Feynman graph calculation, although the identification of p_i in terms of the external and loop momenta depends on the particular time order.

III. RENORMALIZATION

In this section we indicate how to implement the renormalization procedure in TOPTh$_\infty$. This procedure is simple and straightforward to apply in practice, and closely parallels the explicitly covariant Feynman-Dyson approach. Reducible amplitudes with self-energy and vertex insertions are renormalized using subtraction terms corresponding to δ_m, Z_2, and Z_1 counterterms, which usually can be constructed to cancel pointwise the ultraviolet d^2k phase-space integrations. In this section we develop the renormalization procedure for QED in TOPTh$_\infty$ and concentrate on the features which are distinct to the infinite-momentum method. In Sec. IV we discuss the application of these rules to the calculation of the electron anomalous moment in fourth order. Here we present a heuristic proof of the renormalizability of QED and discussion of the uniformity of the $P \to \infty$ limit.

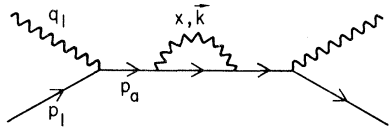

FIG. 4. Feynman graph for a self-energy insertion in the Compton amplitude.

In performing these renormalizations, we are subtracting infinite quantities, which is always a delicate procedure. The correct way to do so is to first regulate the intergrals, rendering them finite, then subtract, and then let the regulators disappear. In the infinite-momentum frame, since covariance is not manifest, one must be especially careful to regulate in an invariant manner. This can be achieved by using the Pauli-Villars regularization scheme.

A. Self-Energy Insertion in Compton Scattering

As a first simple example consider the self-energy insertion to Compton scattering shown in Fig. 4. In the usual Feynman approach the renormalized amplitude is constructed by subtracting formally divergent δ_m and Z_2 counterterms in second order. The problem is to choose an integral representation for these constants so that the total integrand of the renormalized amplitude is finite and pointwise covergent. In general, the integrands are defined assuming covariant Feynman or Pauli-Villars regularization.

The frame is chosen so that the fermion line p_a in Fig. 4 has momentum $\tilde{p}_a = \tilde{P}$. For the moment, consider the case of scalar particles. Only one time-order survives as $P \to \infty$. The unrenormalized amplitude is

$$M_u = \frac{g^4}{2(2\pi)^3} \int d^2k \int_0^1 \frac{dx}{x(1-x)} \left(\frac{1}{s_0 - s_1} \frac{1}{s_0 - s_2} \frac{1}{s_0 - s_3} \right), \tag{3.1}$$

where (using a photon mass λ)

$$\begin{aligned} s_0 &= (p_1 + q_1)^2 + i\epsilon , \\ s_1 &= m^2 = s_3 , \\ s_2 &= \frac{\vec{k}^2 + \lambda^2}{x} + \frac{\vec{k}^2 + m^2}{1-x} . \end{aligned} \tag{3.2}$$

The δ_m and $Z_2 = 1 + B_{(2)}$ counterterm subtractions may be computed by what we call the method of

alternate denominators. Note that δ_m can be written as

$$\delta_m = \frac{g^2}{2(2\pi)^3}\int d^2k \int_0^1 \frac{dx}{x(1-x)} \frac{1}{s_1 - s_2 + i\epsilon} \tag{3.3}$$

since particle a is on the mass shell. (Note this expression must be defined here by covariant-regularization, e.g., by subtraction of a heavy photon of mass Λ^2.) Thus mass renormalization only requires the subtraction of the integrand with the alternate denominator

$$\frac{1}{s_0 - s_1}\frac{1}{s_1 - s_2}\frac{1}{s_0 - s_3} \tag{3.4}$$

in M_u. Similarly, if we perform wave-function renormalization we obtain the renormalized amplitude

$$M_{\text{ren}} = \frac{g^4}{2(2\pi)^3}\int_0^1 dx \int \frac{d^2k}{x(1-x)}\left[\frac{1}{(s_0-s_1)(s_0-s_2)(s_0-s_3)} - \frac{1}{(s_0-s_1)(s_1-s_2)(s_0-s_3)} + \frac{1}{(s_0-s_1)(s_1-s_2)^2}\right]. \tag{3.5}$$

The last term is exactly $-B^{(2)}$ times the Born term. The total integrand is now rendered finite in the ultraviolet ($\vec{k}^2 \to \infty$). By combining the terms, we see that the single-particle poles disappear, so that the location and residue of Compton scattering are still given by the Born term.

The essential point of the "alternate denominator" method is that the external energy used for the denominator of the subtraction term for a reducible insertion is not the external (initial) energy s_0 but rather the energy (s_1) external to that reducible subgraph. The analog to off-mass-shell behavior in the Feynman approach is precisely the difference between the use of s_0 and s_1 in the energy denominators. In general, in self-energy insertions onto a line with momentum $\vec{p}_a$ one should use the "scaled" variables $\vec{l}_1 = x\vec{p}_a + \vec{k}$ and $\vec{l}_2 = (1-x)\vec{p}_a - \vec{k}$ for the internal integration. This will ensure pointwise convergence of the d^2k integration, after subtraction of the necessary counterterms.

Combining terms in M_{ren} we obtain the covariant spectral form

$$M_{\text{ren}} = \frac{g^4}{2(2\pi)^3}\int d^2k \int_0^1 \frac{dx}{x(1-x)} \frac{1}{(s_1-s_2)^2}\frac{1}{s_0-s_2} \tag{3.6}$$

$$= \int_{(m+\lambda)^2}^{\infty} d\mu^2 \rho(\mu^2) \frac{g^2}{(p+q)^2 - \mu^2 + i\epsilon}, \tag{3.7}$$

where $\mu^2 = s_2$ and

$$\rho(\mu^2) = \frac{g^2}{16\pi^2}\frac{1}{(m^2-\mu^2)^2} \times \int_0^1 dx\, \theta(x(1-x)\mu^2 - (1-x)\lambda^2 - x m^2) \tag{3.8}$$

$$= \frac{g^2}{16\pi^2}\frac{1}{(m^2-\mu^2)^2}\frac{[(\mu^2+\lambda^2-m^2)^2 - 4\mu^2\lambda^2]^{1/2}}{\mu^2}. \tag{3.9}$$

Thus the renormalization is identical to that obtained by using the spectral integral of the renormalized Feynman propagator, since

$$\pi\rho(\mu^2) = \text{Im} D_F^{\text{ren}}(\mu^2).$$

B. Vacuum Polarization

Consider the vacuum-polarization insertion in electron-electron scattering [Fig. 5(a)]. If we choose a frame in which $\vec{q} = \vec{p}_1 - \vec{p}_2$ has a positive component along $\vec{P}$, then only the time order in which the (q, p_1, p_2) vertex occurs first and the (q, p_3, p_4) vertex occurs last contributes for $P \to \infty$. The energy denominator for any intermediate state inside the vacuum-polarization insertion is

$$\frac{1}{E_1 + E_3 - \left(E_2 + E_3 + \sum_{\text{vac.pol.}} E_i\right)} = \frac{1}{E_1 - E_2 - \sum_{\text{vac. pol.}} E_i}, \tag{3.10}$$

so that the initial energy for the vacuum-polarization insertion is $\tilde{q}_0 \equiv p_1^0 - p_2^0$. Thus if we define $q_F^2 = (p_1 - p_2)^2$, then the amplitude has the factorized Feynman form

$$M = g^2 \frac{1}{(q_F^2 - \lambda^2 + i\epsilon)^2}\pi_u(q_F^2), \tag{3.11}$$

where $\pi_u(q_f^2)$ is computed from diagram 5(b), for a photon mass $q_F^2 < 0$. The Feynman propagator $q_F^2 - \lambda^2 + i\epsilon$ is obtained from the product of the photon phase space $(2q_0)^{-1}$ and the energy denominator

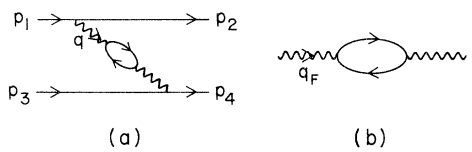

FIG. 5. (a) Vacuum-polarization contribution to particle scattering. (b) Vacuum-polarization insertion calculated in Eq. (3.19).

$(p_{10}-p_{20}-q_0+i\epsilon)^{-1}$ at infinite momentum.

Renormalization may now be carried out by the alternate denominator method as in Sec. III A. The renormalized amplitude is then a spectral integral of the Born amplitude over photon mass which we shall calculate below. We can easily extend the analysis to self-insertion in higher-order graphs. For example, consider the time-ordered contributions to electron-electron scattering shown in Fig. 6. After the integrand for the counterterms for the vacuum polarization insertion is computed using the alternate energy denominator method, one finds that the three time orders combine simply and the renormalized amplitude can again be written as the spectral integral in photon mass over the "Born" amplitude of Fig. 7.

As a further example, we calculate the lowest-order vacuum polarization correction to lepton-lepton scattering in QED. The sum of the contributions from Fig. 8 is

$$l_1^{\alpha} l_2^{\beta}\left[\frac{-g_{\alpha\beta}}{q_F^{\,2}+i\epsilon}+\frac{(-g_{\alpha\mu})(-g_{\nu\beta})}{(q_F^{\,2}+i\epsilon)^2}\pi^{\mu\nu}\right], \tag{3.12}$$

where by Lorentz invariance $\pi^{\mu\nu}$ is a function of $q_F^{\mu}=p_1^{\mu}-p_2^{\mu}$ and by gauge invariance $\pi^{\mu\nu}$ has the form

$$\pi^{\mu\nu}=(-g^{\mu\nu}q_F^{\,2}+q_F^{\mu}q_F^{\nu})\pi(q^2) \tag{3.13}$$

and l_1 and l_2 are the lepton current factors. At infinite momentum we can extract $\pi(q^2)$ from $\pi_{\mu\nu}$ simply by considering

$$\pi_{03}=q_0 q_3 \pi(q^2). \tag{3.14}$$

Moreover, choosing

$$q=\left(P+\frac{q^2}{2P},\vec{0},P\right), \tag{3.15}$$

we see that

$$\pi(q^2)=\lim_{P\to\infty}\frac{\pi_{03}(q^2)}{P^2}. \tag{3.16}$$

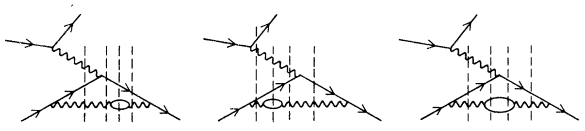

FIG. 6. Time-ordered contributions corresponding to the vacuum-polarization insertion in a vertex correction to electron-electron scattering. The three time orders combine, when renormalized, to the renormalized covariant photon propagator modification for Fig. 7.

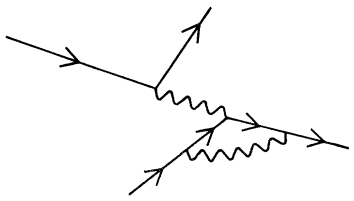

FIG. 7. Vertex correction to electron-electron scattering.

Only the piece of π_{03} proportional to P^2 survives, and graph 8(c) is eliminated. Restricting our attention to graph 8(b), we have

$$\pi_{03}=\frac{e^2}{2(2\pi)^3}\int_0^1 dx\int\frac{d^2k}{x(1-x)}\,\mathrm{Tr}[(m+\not p_1)\gamma^0(m-\not p_2)\gamma^3]\times\left(q_F^{\,2}-\frac{\vec{k}^2+m^2}{x}\,\frac{\vec{k}^2+m^2}{1-x}+i\epsilon\right)^{-1}, \tag{3.17}$$

where p_1 and p_2 are on-shell with space components $(\vec{k}, xP)$ and $(-\vec{k}, (1-x)P)$, respectively. The term proportional to P^2 gives the unrenormalized amplitude

$$\pi(q_F^{\,2})=\lim_{P\to\infty}\frac{\pi_{03}}{P^2}=\frac{4e^2}{(2\pi)^3}\int_0^1 dx\int d^2k\,\frac{x(1-x)}{\vec{k}^2+m^2-q_F^{\,2}x(1-x)-i\epsilon}. \tag{3.18}$$

We obtain the renormalized amplitude by subtraction at $q^2=0$ (corresponding to wave-function renormalization of the photon) or by alternate denominators. Thus

$$\pi_{\mathrm{ren}}(q_F^{\,2})=\frac{2\alpha}{\pi}\int_0^1 dx\,x(1-x)\ln\left[1-\frac{q_F^{\,2}x(1-x)}{m^2-i\epsilon}\right] \tag{3.19}$$

and the total lepton-lepton scattering interaction for Fig. 8 is

$$l_1^{\mu}l_2^{\nu}\frac{(-g_{\mu\nu})}{q_F^{\,2}-\lambda^2+i\epsilon}[1+\pi_{\mathrm{ren}}(q^2)] \tag{3.20}$$

in agreement with the standard results.

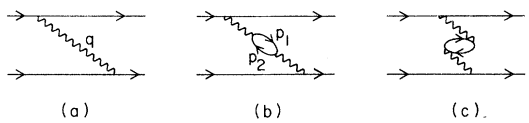

FIG. 8. Contribution to electron-electron scattering from time-ordered perturbation theory.

C. Vertex Factorization

Before discussing vertex renormalization, we first give a general proof of vertex factorization in TOPTh. Consider the scattering diagram of Fig. 9 in which the vertex part contains a total of $N+1$ internal interactions. For simplicity we continue to treat all the particles as spinless.

We choose q to have positive momentum in the $\vec{P}$ direction. If q attaches to an internal line after m internal interactions have occurred ($0 \leq m \leq N$), then there are $m+1$ contributing time orders depending on the time of the (p_1, p_2, q) interaction. Since q is on the mass shell, $q_0 = (\vec{q}^2+\lambda^2)^{1/2}$. We also define $\tilde{q}_0 = p_1^0 - p_2^0 = p_4^0 - p_3^0$. Summing over the $m+1$ contributions yields the integrand factor

$$
\begin{aligned}
F_m = & \frac{1}{\tilde{q}_0 - q_0} \frac{1}{\tilde{q}_0 + \Delta e_1 - q_0} \frac{1}{\tilde{q}_0 + \Delta e_2 - q_0} \cdots \frac{1}{\tilde{q}_0 + \Delta e_m - q_0} \\
& + \frac{1}{\Delta e_1} \frac{1}{\tilde{q}_0 + \Delta e_1 - q_0} \frac{1}{\tilde{q}_0 + \Delta e_2 - q_0} \cdots \frac{1}{\tilde{q}_0 + \Delta e_m - q_0} \\
& + \frac{1}{\Delta e_1} \frac{1}{\Delta e_2} \frac{1}{\tilde{q}_0 + \Delta e_2 - q_0} \cdots \frac{1}{\tilde{q}_0 + \Delta e_m - q_0} \\
& + \cdots + \frac{1}{\Delta e_1} \frac{1}{\Delta e_2} \cdots \frac{1}{\Delta e_m} \frac{1}{\tilde{q}_0 + \Delta e_m - q_0} \\
= & \frac{1}{\tilde{q}_0 - q_0} \prod_1^m \frac{1}{\Delta e_j} ,
\end{aligned}
\tag{3.21}
$$

where Δe_i is the ith energy denominator specific to the vertex. The remaining energy denominators give the common factor

$$
\prod_{j=m+1}^{N} \frac{1}{\Delta e_j + \tilde{q}_0} . \tag{3.22}
$$

The phase-space factor for the photon $2q_0$ combines with the factor $(\tilde{q}_0 - q_0)$ to give the Feynman propagator,

$$
\begin{aligned}
2q_0(\tilde{q}_0 - q_0) &= (p_1 - p_2)^2 - \lambda^2 + i\epsilon \\
&\equiv q_F^{\,2} - \lambda^2 + i\epsilon .
\end{aligned}
\tag{3.23}
$$

Thus, as expected, for each m the scattering amplitude takes the Feynman factorized form

$$
M = \frac{g}{\tilde{q}^2 - \lambda^2 + i\epsilon} F(\tilde{q}^2) , \tag{3.24}
$$

where $F(\tilde{q}^2)$ is the vertex graph computed with the photon mass given formally by $\tilde{q}^2 = (p_1 - p_2)^0 < 0$. Note that pair creation graphs also have the form (3.24).

Thus, the concept of virtual-mass particles and the factorization of vertex form factors appears naturally in TOPTh when the appropriate time orders are summed over. This also permits by covariance the use of the special frame choice[4]

$$
\begin{aligned}
& q^\mu = (q \cdot p/P, \vec{q}, 0), \quad q^2 = -\vec{q}^2 < 0 \\
& p = (P + m^2/2P, \vec{0}, P)
\end{aligned}
\tag{3.25}
$$

which is very convenient for calculations of the virtual Compton amplitude ($q \cdot p = m\nu$) and form factor ($2q \cdot p = -q^2$). In this frame, $\vec{q}$ brings in zero longitudinal momentum, eliminates pair-creation graphs, and thus further reduces the number of contributing time orders.

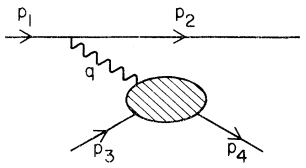

FIG. 9. General vertex correction to electron-electron scattering. When all internal time-ordered contributions are combined, the covariant vertex correction (3.24) results.

D. Ward Identity

The use of frame (3.25) allows an immediate proof of the Ward identity $Z_1 = Z_2$ for the cancellation of vertex and wave-function renormalization in QED. We define the form factors as

$$
\begin{aligned}
& \langle p+q | J^\mu(0) | p \rangle \\
& = \bar{u}(p+q) \left(F_1(q^2) \gamma^\mu + i \frac{\sigma^{\mu\nu} q_\nu}{2m} F_2(q^2) \right) u(p) .
\end{aligned}
\tag{3.26}
$$

At $t = 0$ we may identify $J_\mu(0) = j_\mu(0) = :\bar{\psi}\gamma_\mu\psi:$, the free current, in the interaction picture, and compute F_i by TOPTh. Let us concentrate here on computing the contribution to Z_1 or $F_1(0)$ from any given proper vertex diagram in TOPTh. Note that for $q = 0$

$$
F_1(0) = \lim_{P \to \infty} \langle p | j_\mu(0) | p \rangle \frac{m}{P} \quad (\mu = 0, 3) . \tag{3.27}
$$

Thus the contribution to Z_1 from any proper vertex graph is obtained by simply inserting $(m/P)\gamma_0$ or equivalently x at the interaction vertex, where x is the fractional longitudinal momentum of the interacting charged line. This factor of x cancels against one of the two phase-space forms of x^{-1} required for that line. The resulting expression is then identical to that required for computing the contribution of the corresponding proper diagram to the wave-function renormalization constant Z_2 for the state $|p\rangle$. The result $Z_1 = Z_2$ then holds to

our order in perturbation theory. The same simple proof holds in the case where $|p\rangle$ is a bound state.

E. Vertex Renormalization

As a final simple example of the alternate-denominator renormalization procedure in QED, consider the renormalization of the vertex insertion in the ladder-graph contribution to the electron anomalous magnetic moment $F_2(0)$. If we choose the (symmetrized) frame

$$q^\mu=(0,\vec{q},0),$$

$$(p\pm\tfrac{1}{2}q)=\left(P+\frac{m^2+\frac{1}{4}\vec{q}^2}{2P},\pm\tfrac{1}{2}\vec{q},P\right),$$

$$q^2=-\vec{q}^2,$$

then only the single time order shown in Fig. 10 needs to be explicitly considered at $P\to\infty$. [Recall that backward-moving fermion contributions are included automatically by modifying the fermion spin sum (2.17).] As in the Feynman calculation the integration of the reducible subgraph is logarithmically divergent in the ultraviolet. The subtraction of the contribution $(\alpha/2\pi)L^{(2)}$ is required, where $\gamma_\mu L^{(2)}$ is the value of the proper vertex at $q=0$ in second order. The unrenormalized amplitude is

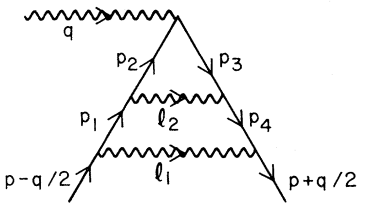

FIG. 10. Labeling of the two-photon ladder-graph contribution to the electron vertex.

$$M_u=\frac{e^4}{4(2\pi)^6}\int_0^1 dx_1dx_2\int\frac{d^2k_1d^2k_2}{x_1(1-x_1)^3x_2(1-x_2)^2}$$

$$\times\frac{\bar{u}(p+\frac{1}{2}q)\gamma_\alpha(\gamma\cdot\tilde{p}_4+m)\gamma_\beta(\gamma\cdot\tilde{p}_3+m)\gamma_\mu(\gamma\cdot\tilde{p}_2+m)\gamma^\beta(\gamma\cdot\tilde{p}_1+m)\gamma^\alpha u(p-\frac{1}{2}q)}{(s_0-s_1)(s_0-s_2)(s_0-s_3)(s_0-s_4)}, \tag{3.28}$$

where we choose the parameterization

$$\vec{l}_1=\vec{k}_1+x_1\vec{P},$$

$$\vec{l}_2=\vec{k}_2+x_2[-\vec{k}_1+(1-x_1)\vec{P}]$$

for the three-momentum of the two photons. The fermion momenta then are determined by three-momentum conservation. With this choice of scaled variables the range of both x_1 and x_2 is 0 to 1 and $\vec{k}_1\cdot\vec{k}_2$ cross terms do not appear. Notice that the denominator product in (3.28) is an even function of $\vec{q}$ because of the choice of the symmetrized frame. In the calculation of $F_2(0)$, the magnetic-moment contribution is identified[12] from a term linear in $\vec{q}$ and the $\vec{q}$ dependence of the denominators may be dropped.

The subtraction term is constructed using the alternate denominators $(s_1-s_2)(s_1-s_3)$ instead of $(s_0-s_2)(s_0-s_3)$ and the appropriate numerator coefficient of γ_μ at $q\to0$:

$$M_{\rm sub}=\frac{e^4}{4(2\pi)^6}\int_0^1 dx_1dx_2\int\frac{d^2k_1d^2k_2}{x_1(1-x_1)^3x_2(1-x_2)^2}$$

$$\times\frac{\bar{u}(p+\frac{1}{2}q)\gamma_\alpha(\gamma\cdot\tilde{p}_4+m)\gamma_\mu(\gamma\cdot\tilde{p}_1+m)\gamma^\alpha u(p-\frac{1}{2}q)}{(s_0-s_1)(s_0-s_4)}\left[\frac{(8m^2-4p_1\cdot p_2)(1-x_2)}{(s_1-s_2)(s_1-s_3)}\right]_{q\to0}. \tag{3.29}$$

The last factor is the integrand for $L^{(2)}$ in second order. The difference

$$M_{\rm ren}=M_u-M_{\rm sub}$$

converges pointwise in the d^2k integrations, and contributes a finite amount to $F_2(0)$. The infrared behavior [at $x_1\sim0$ in M_u and $x_2\sim0$ in $M_{\rm sub}$] may be regulated by using a finite photon mass λ as in the Feynman calculation. In the case of the ladder-graph contribution to $F_2(0)$, these two infrared terms in fact cancel. The cancellation may be arranged to happen pointwise in the integrand by symmetrizing the $(\vec{k}_1,x_1)$ and $(\vec{k}_2,x_2)$ integration of $M_{\rm ren}$.

F. The Renormalization Constants

The calculation of δm_e in second order is an excellent illustration of the subtleties of the limit $P\to\infty$. As we have already indicated, our rule for incorporating fermions of negative x is not valid in this case, so we revert to the older rules in which particles of negative x are treated explicitly. Then there are two graphs, as indicated in Figs. 11(a) and 11(b). As is well known these graphs are divergent and have to be regulated. A naive argument would say that, upon photon regularization, graph 11(b) vanishes, for since at least one of the particles in the intermediate state has $x<0$, the energy denominator is just $1/(1-\sum_{\text{int}}|x_i|)$ independent of the photon mass. Consequently, subtracting a similar integrand with a large photon mass will give identically zero.

Unfortunately, the argument is wrong, because the limit $P\to\infty$ cannot be taken under the integral sign. One must integrate first, and only then let $P\to\infty$.

To see this, let us define the $P\to\infty$ rules more carefully. Ignoring the numerator structure for the moment, the denominators are, before we take $P\to\infty$,

$$\frac{1}{e_k}\,\frac{1}{E_{-p-k}}\,\frac{1}{E-e_k-E_{-p-k}}\,, \tag{3.30}$$

where

$$\begin{aligned} e_k&=[(xP)^2+\vec{k}^2+\lambda^2]^{1/2},\\ E_{-p-k}&=[(1-x)^2P^2+\vec{k}^2+m^2]^{1/2},\\ E&=(P^2+m^2)^{1/2}, \end{aligned} \tag{3.31}$$

and λ is a small photon mass.

For large P we wrote

$$e_k=|x|P+\frac{\vec{k}^2+\lambda^2}{2|x|P} \tag{3.32}$$

and disregarded the second term in (3.32) in the first term of (3.30). This is legitimate provided that the function multiplying $1/e_k$ vanishes at $x=0$, so that the integral over x is well defined. In other words as a distribution on functions vanishing at $x=0$ we have

$$\frac{1}{e_k}\to\frac{1}{|x|P} \tag{3.33}$$

for large P. But if the functions vanish at $x=0$, we could also write

$$\frac{1}{e_k}\to\frac{1}{|x|P}+\frac{C\delta(x)}{P}\,. \tag{3.34}$$

To fix the coefficient C, consider what happens if the function does not vanish at $x=0$. Then the integral is not well defined and must be regulated,

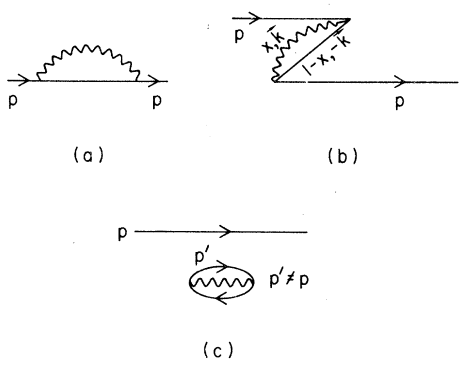

FIG. 11. Time-ordered contribution to the electron self-energy. Because of the Pauli principle (c) contributes instead of (b) when $p'=p$.

by subtracting the contribution of a heavy photon. So we must study

$$\lim_{P\to\infty}\frac{P}{[(xP)^2+\vec{k}^2+\lambda^2]^{1/2}}-\frac{P}{[(xP)^2+\vec{k}^2+\Lambda^2]^{1/2}}\,, \tag{3.35}$$

where Λ is the mass of the regulator photon. For $x\neq 0$ this limit vanishes. But it is readily checked that as a distribution in x, (3.35) tends to

$$-\ln\left(\frac{\vec{k}^2+\lambda^2}{\vec{k}^2+\Lambda^2}\right)\delta(x)\,. \tag{3.36}$$

This is consistent with (3.34) if

$$C=-\ln(\vec{k}^2+\lambda^2). \tag{3.37}$$

One might argue that

$$\frac{P}{e_k}=\frac{1}{[x^2+(\vec{k}^2+\lambda^2)/P^2]^{1/2}} \tag{3.38}$$

is not a function of $(k^2+\lambda^2)$, but of $(\vec{k}^2+\lambda^2)/P^2$, so that C should be $-\ln[(\vec{k}^2+\lambda^2)/P^2)]$. But on regularization the $\ln P^2$ terms cancel. Using then as the energy term

$$\frac{P}{e_k}=\frac{1}{|x|}-\ln(\vec{k}^2+\lambda^2)\delta(x) \tag{3.39}$$

one shows that (11b) does give a contribution upon regularization.

By our rules after regularization the contribution of diagram 11(a) to δm is

$$\delta m_a=\frac{e^2}{16\pi^3 m}\int d^2k\int_0^1\frac{dx}{1-x}\left[\frac{m^2(2-2x-x^2)-\vec{k}^2}{\lambda^2(1-x)+\vec{k}^2+m^2x^2}-(\lambda\to\Lambda)\right], \tag{3.40}$$

where the photon mass is taken to be λ, and its longitudinal and transverse momenta are xP and $\vec{k}$.[13]

Our new rule for δm_b gives

$$\delta m_b = -\frac{e^2}{16\pi^3 m}\int d^2k[\ln(\vec{k}^2+\lambda^2)-\ln(\vec{k}^2+\Lambda^2)]\,. \tag{3.41}$$

Combining these two terms yields the Feynman result, which can be written as

$$\delta m_F = \frac{e^2}{16\pi^3 m}\int d^2k\int_0^1 dx\left[\frac{2m^2(1+x)}{\vec{k}^2+m^2x^2+(1-x)\lambda^2} -(\lambda\longrightarrow\Lambda)\right]. \tag{3.42}$$

This can be obtained by substituting the identity

$$\ln(\vec{k}^2+\lambda^2)-\ln(\vec{k}^2+\Lambda^2)=\ln\left(\frac{\vec{k}^2+\lambda^2}{\vec{k}^2+m^2}\right)-\ln\left(\frac{\vec{k}^2+\Lambda^2}{\vec{k}^2+m^2}\right) =\int_0^1\left[\frac{\lambda^2-2m^2x}{\vec{k}^2+m^2x^2+(1-x)\lambda^2} -(\lambda\longrightarrow\Lambda)\right]dx \tag{3.43}$$

into δm_b. Another derivation of this result is given in the Appendix.

It is clear that for amplitudes which are already finite, the $\delta(x)$ cannot contribute and our previous rules are correct. Thus, for example, in calculating the contribution of Fig. 12 (and the corresponding δ_m counterterms of Fig. 13) to the magnetic moment of the electron, the contributions of Figs. 12(b) and 13(b) cancel identically upon regularization. For renormalized amplitudes only Fig. 11(a) contributes to the self-energy insertion.

It should be noted that technically, if the Pauli principle were taken into account, graph 11(b) would not contribute to δ_m since the intermediate state has two electrons of the same momentum and spin. In fact, the actual contribution of interest is the vacuum disconnected graph 11(c), where the entire Fig. 11(c) d^4p integration would give no physical contribution, except for the fact that the

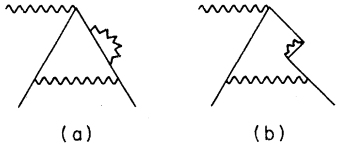

FIG. 12. Time-ordered contributions for a self-energy correction to the electron vertex.

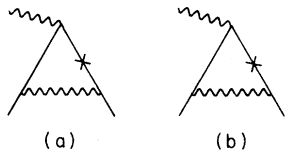

FIG. 13. Mass-shift subtraction terms for the two time-ordered self-energy contributions of Fig. 12, corresponding to Eqs. (3.40) and (3.41), respectively.

$p'=p$ contribution is missing. However, 11(c) gives the same contribution as 11(b) calculated as if the Pauli principle is ignored. This is clear since we can imagine taking the final momentum equal to $p+\delta$ in 11(b) by considering an off-shell process. The sum of 11(b) and 11(c) is continuous as $\delta\to 0$. Accordingly we can follow the usual Feynman convention of ignoring the Pauli principle and the contribution of vacuum disconnected amplitudes. In the case of the unrenormalized amplitude for the vertex graph of Fig. 14, a $\delta(1-x)$ contribution will occur. (This disagrees with the argument given in Ref. 5, that all distribution-type terms can be associated with vacuum disconnected graphs.) However, upon regularization in the photon mass this contribution cancels, and it never appears in the renormalized amplitude. We note also that if regularization in the lepton mass is used in the δ_m calculation, then $\delta(x)$ contributions may be formally ignored.

G. Renormalizability

It is possible to give a heuristic proof of renormalizability of various theories directly from TOPTh in the infinite-momentum frame. The ultraviolet divergences of the phase-space integrations are assumed to be covariantly regulated by gauge-invariant Pauli-Villars negative-metric internal leptons or photons (or by Feynman spectral conditions) where required. The infrared behavior at $x_{\text{photon}}\sim 0$ may be regulated by using a photon mass λ^2.[14] We use the Weinberg power-counting theorem.[15] After removal of divergent subgraphs, the phase-space integrals of the skeleton graph will converge in the ultraviolet if the total degree of divergence d is negative.

We begin with the ϕ^3 theory. Recall that the degree of divergence in the Feynman theory is, for a graph with V vertices and N internal lines,

$$4N-2N-4(V-1)\,,$$

where $4N$ comes from d^4k, $-2N$ from the propagators, and $-4(V-1)$ from momentum conservation, while in our rules it is

$$2N-2(V-1)-2(V-1),$$

where $2N$ comes from d^2k, $-2(V-1)$ from energy denominators, and $-2(V-1)$ from momentum conservation, which agrees with the Feynman result. Thus, just as in the Feynman case, one proves the renormalizability of the theory.

For any Feynman diagram in spin-$\frac{1}{2}$ QED, one finds from the usual Feynman rules

$$d_{1/2}=4(B_i+F_i)-(F_i+2B_i)-4(V-1)$$
$$=4-\tfrac{3}{2}F_e-B_e,$$

where $4(B_i+F_i)$ comes from d^4k, $-(F_i+2B_i)$ from propagators, and $-4(V-1)$ from momentum conservation, where B_i, B_e, F_i, and F_e denote the number of internal and external bosons and fermions.[16] For spin-zero electrodynamics, we have

$$d_0=4(B_i+F_i)+V-(2F_i+2B_i)-4(V-1)$$
$$=4-F_e-B_e,$$

where $4(B_i+F_i)$ comes from d^4k, V from numerator terms, $-(2F_i+2B_i)$ from propagators, and $-4(V-1)$ from momentum conservation.

The only difficulty in deriving analogous rules for spin-$\frac{1}{2}$ QED in TOPTh$_\infty$ is in deciding the number of powers of k contributed by the spin sums $\not{p}_i+m_i$ or $\gamma\cdot\tilde{p}_i+m_i$. For each internal fermion line, these spin sums contribute one power of $|\vec{k}|$ from $\vec{\gamma}\cdot\vec{k}$. If any two of these internal vectors dot together, this rule is correct since the result is of order $\vec{k}^2$. If, however, such a p_i dots with an external line, the contribution is of order $\vec{k}^2$, not $|\vec{k}|$. We now show that this can contribute at most an extra factor $|\vec{k}|^{F_e/2}$.

This situation arises in computing

$$\bar{u}(p'')\mathfrak{M}u(p'),$$

where p', p'' are external fermion momenta and $\mathfrak{M}$ is formed from scalars and $\not{p}_i$. It can be verified that the combination

$$p_1\cdot p''\,p_2\cdot p'$$

cannot occur in such a term, except in the combination

$$(p_1\cdot p''\,p_2\cdot p'-p_2\cdot p''\,p_1\cdot p')$$

which is at most of order $\vec{k}^3$, and not of order $\vec{k}^4$. This is a reflection of the fact that two spin-$\frac{1}{2}$ spinors (of momentum p', p'') cannot couple to a spin-2 object, as is required to produce the *symmetric* tensor $p'_\mu p'_\nu$. As a result, for each two external fermions, the degree of $\vec{k}$ in the matrix element can only be increased by 1. A similar rule holds for the $\gamma_0 p_0$ terms. Thus the powers of $\vec{k}$ contributed by the spin sums is at most

$$F_i+\tfrac{1}{2}F_e.$$

Then we obtain, for each time-order diagram in spin-$\frac{1}{2}$ QED, the degree of divergence

$$d_{1/2}=2(B_i+F_i)+(F_i+\tfrac{1}{2}F_e)-2(V-1)-2(V-1)$$
$$=4-F_e-B_e,$$

where $2(B_i+F_i)$ comes from d^2k_i, $(F_i+\frac{1}{2}F_e)$ from the numerator terms, $-2(V-1)$ from the energy denominators, and $-2(V-1)$ from momentum conservation.

Similarly, for spin-0, TOPTh QED at infinite momentum

$$d_0=2(B_i+F_i)+V-2(V-1)-2(V-1)$$
$$=4-F_e-B_e,$$

where $2(B_i+F_i)$ comes from d^2k_i, V from the numerator terms, $-2(V-1)$ from the energy denominators, and $-2(V-1)$ from momentum conservation. Since d depends on the number of external lines, there are a finite number of divergent subgraphs and the usual renormalization program may be carried out. Note that the result for $d_{1/2}$ is an overestimate since, as the Feynman result shows, the extra $\frac{1}{2}F_e$ in $d_{1/2}$ cancels when the various time orderings are combined.

This cancellation (between pair states and nonpair states) can be traced to Fermi statistics.

H. Convergence as $P\to\infty$

We restrict our attention to ϕ^3 theories. We have already shown in Sec. III G that the degree of divergence in $\vec{k}^2$ is as in the Feynman theories, and it is easily seen that there is no divergence in x, since the factor $1/x$ associated with each line is compensated by the factor $(\vec{k}^2+m^2)/x$ appearing in the energy denominator of the intermediate states in which this line occurs.

We discarded contributions of particles with negative x because the energy denominators formally suppressed the graph by $1/P^2$. But the effective energy denominator

$$\frac{1}{P^2}\,\frac{1}{1-\sum_{\text{int}}|x_i|}$$

does not contain the factor x/k^2 which we counted on in our previous analysis, so that one could get divergence at $x=0$ or $k^2=\infty$. To study these recall that the energy denominator is really

$$\frac{1}{P^2}\left(1-\sum|x_i|+\sum_{\text{inc}}\frac{\vec{k}_i^{\,2}+m_i^{\,2}}{2x_iP^2}-\sum_{\text{int}}\frac{\vec{k}_i^{\,2}+m_i^{\,2}}{2|x_i|P^2}\right)^{-1}. \tag{3.44}$$

If only x_1 is negative, then as it goes to zero the term is

$$\frac{1}{P^2}\,\frac{1}{2x_1+O(1/x_1P^2)}. \tag{3.45}$$

The $O(1/x_1P^2)$ term cuts off the integral at $x_1 = O(1/P)$. The contribution to the graph from small x_1 is then

$$\frac{1}{P^2}\int_{|x_1|>1/P}\frac{dx_1}{|x_1|}\,\frac{1}{2x_1}\approx O(1/P) \tag{3.46}$$

and so is still negligible. By a similar argument the $\vec{k}^2$ integral is cut off at P^2 (actually $\vec{k}^2=xP^2$). If the rest of the graph contributes a factor $1/\vec{k}^2$ then the entire contribution is

$$\frac{1}{P^2}\int_{\vec{k}^2<P^2}\frac{d^2k}{\vec{k}^2}=\frac{-\ln P^2}{P^2}\ , \tag{3.47}$$

which is still negligible. However, if there is no other factor $1/\vec{k}^2$ the graph contributes

$$\frac{1}{P^2}\int_{\vec{k}^2<P^2}d^2k=O(1) \tag{3.48}$$

and is *not* negligible. This only happens if the vector k does not occur in any other intermediate state, for otherwise the energy denominator of that state would have a factor $1/\vec{k}^2$. But this can only happen in the lowest-order self-energy graphs or in any graph in which these are imbedded. These are self-energy terms which must be regulated anyway, by subtracting the contribution of a heavy mass M. One verifies that after regularization the contribution of negative x can be discarded.

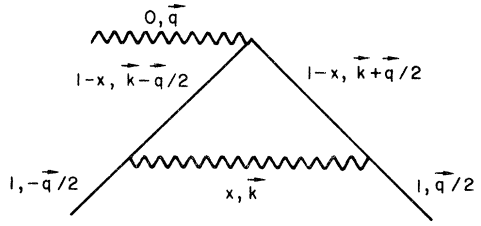

FIG. 14. Labeling of the vertex diagram for the anomalous moment calculation.

In summary, our $P=\infty$ rules are valid for renormalized quantities but not for unrenormalized ones.

IV. CALCULATIONS

As an example of these techniques, we have calculated the 4th-order contribution to the magnetic moment of the electron in QED. We chose this particular calculation because it involves all three types of renormalization, and agreement between our answers and the well-known results of Sommerfield and Petermann[17] would be confirmation that both the $P\to\infty$ limit and the renormalizations were correctly handled. We also hoped that our techniques would prove competitive with the Feynman approach, so that we could proceed to calculate part of the 6th-order moment. We begin with the calculation of the second-order anomalous moment.[18] Consider the graph shown in Fig. 14, in which the external photon has $x=0$ and polarization index 0. x and $\vec{k}$ are labeled for each line. By our rules the matrix element, without external fermion spinors, is

$$\mathfrak{M}=-\frac{e^2}{2(2\pi)^3}\int\frac{d^2k\,dx}{x(1-x)^2}\,\gamma^\mu(\not p_1+m)\gamma^0(\not p_2+m)\gamma_\mu$$
$$\times\left(m^2+\tfrac{1}{4}\vec{q}_\perp^{\,2}-\frac{\vec{k}^2}{x}-\frac{(\vec{k}-\frac{1}{2}\vec{q})^2+m^2}{1-x}\right)^{-1}\left(m^2+\tfrac{1}{4}\vec{q}_\perp^{\,2}-\frac{\vec{k}^2}{x}-\frac{(\vec{k}+\frac{1}{2}\vec{q})^2+m^2}{1-x}\right)^{-1}, \tag{4.1}$$

where p_1, p_2 are on-shell vectors with space components $(\vec{k}+\frac{1}{2}\vec{q}, (1-x)P)$ and $(\vec{k}-\frac{1}{2}\vec{q}, (1-x)P)$.

It is readily verified that the anomalous moment is obtained from $\mathfrak{M}$ by

$$F_2(0)=\lim_{q\to\infty}\lim_{P\to\infty}\frac{2m^2}{4}\,\mathrm{Tr}\frac{[\mathfrak{M}(\not p-\frac{1}{2}\not q+m)(\gamma^0/P-1/m)(\not p+\frac{1}{2}\not q+m)]}{-q^2P}\ , \tag{4.2}$$

where $p-\frac{1}{2}q$, and $p+\frac{1}{2}q$ are on-shell vectors with space components $(-\frac{1}{2}\vec{q}, P)$ and $(\frac{1}{2}\vec{q}, P)$, respectively.

Performing the trace and taking the appropriate limits we obtain

$$F_2(0)=2m^2\frac{e^2}{(2\pi)^3}\int_0^1 dx\,x^2(1-x)\int d^2k\frac{1}{(\vec{k}^2+m^2x^2)^2}$$
$$=2m^2\frac{e^2}{(2\pi)^3}\int_0^1 dx\frac{1-x}{m^2}\,\pi=\frac{\alpha}{2\pi}\ .$$

In the lowest-order calculations the x variable plays the role of the Feynman denominator-combining parameter. This identification, however, cannot be made in general.

There are five different Feynman graphs contributing to the magnetic moment in fourth order. They are shown together with the corresponding time-ordered graphs in Fig. 15. As explained in Sec. II, it is sufficient to consider only those time orderings with all $x_1 > 0$.

We wrote a two-stage program to perform these calculations. The first stage was a symbolic and algebraic program written in REDUCE.[19] It took as input the topology of the Feynman graph, and automatically generated the surviving time orders, set up and performed the required traces, computed the energy denominators, and expressed everything in terms of the infinite-momentum-frame variables. The output is a set of FORTRAN expressions, which served as input to the second stage, a multidimensional integration program written by Sheppey.[20] The vacuum-polarization graph was handled as indicated in Sec. III. As independent variables for the crossed and corner graphs, we used x and $\vec{k}$ for each of the two virtual photons. In the ladder and self-energy graphs, we parametrized the momenta of the photons as follows:

(1) outer photon: $x = x_1$, $\vec{k} = \vec{k}_1$,

(2) inner photon: $x = x_2(1-x_1)$, $\vec{k} = \vec{k}_2 - x_2\vec{k}_1$.

With this choice, x_2 ranges between 0 and 1 and the energy denominators have no terms in $\vec{k}_1 \cdot \vec{k}_2$. This made the integrals over the directions $\vec{k}_1$ and $\vec{k}_2$ trivial, so that the resulting integrals were four-dimensional (over x_1, x_2, $\vec{k}_1^{\,2}$, $\vec{k}_2^{\,2}$), while those of the crossed and corner graphs were five-dimensional.[21]

The crossed graph can be computed immediately,[22] since it requires no renormalization. The renormalization of the ladder and self-energy graphs were straightforward, as outlined in Sec. III. The infrared piece of the ladder graph canceled after symmetrizing the integrand in $(x_1, \vec{k}_1^{\,2})$ and $(x_2, \vec{k}_2^{\,2})$, while the infrared piece of the self-energy graph was removed as in the Feynman method.

The only difficult graph to renormalize was the corner graph. Until this point, our representation for the counterterms assured that the divergence (in the $\vec{k}$ integral) of the unrenormalized graph and the counterterms canceled pointwise. In the corner graph, both IV(a) and IV(b) required subtraction. (See Fig. 15.) Although the divergence of both graphs adds up to that of the counterterm, we

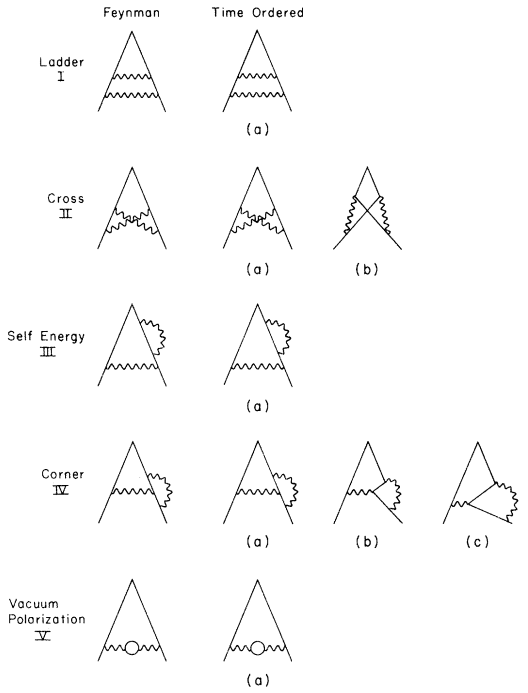

FIG. 15. Contributions to the order-α^2 corrections to the electron vertex. The left column shows the Feynman graph. The other columns display the corresponding essential time-ordered contributions as $P \to \infty$.

did not find an elegant representation of the counterterm $(\alpha/2\pi) \times L^{(2)}$ which renders each time order finite. What we did was to isolate the divergent pieces of each time order, and analytically compute the difference between these terms and the counterterms, using a regulator photon mass to assure covariance. Covariant regularization was essential in obtaining the right answer, since the subtraction of two divergent quantities is ambiguous. Our method in this graph was similar in spirit to intermediate renormalization[23] in standard QED calculations in which subtraction terms, differing from the usual counterterms, but with the same ultraviolet behavior, are introduced in intermediate stages of the calculation.

It should be noted that even for these graphs, our integrand was given by the infinite-momentum-frame rules. It was not necessary to renormalize at finite momentum and then take the infinite-momentum limit.

To understand the origin of the difficulty in renormalizing the corner graph, recall that the photon incident on the reducible vertex piece has $x \neq 0$, whereas in the counterterm the photon is taken to have $q_\mu = 0$. Thus in the counterterm an insertion like that depicted in Fig. 16 cannot appear, since a photon with $x = 0$ cannot produce two fermions with positive x. Nevertheless, the main

graph IV(b) containing this insertion diverges. The lines external to the reducible insertions in IV(b) do not satisfy energy conservation. Thus, the insertion is not Lorentz-invariant, and it can be verified that graph IV(b) is finite in TOPTh in a frame with finite momentum. It is the limit $P\to\infty$ which gives rise to the divergence. This is of course possible, since the noninvariant insertion is frame-dependent.

The results of our calculations agreed with the usual answers.[17] But as a pleasant surprise, it appeared that our integrands, expressed as a function of x_i and $\vec{k}_i$, are smoother than the corresponding usual integrands expressed as a function of the Feynman parameters. As a result, the numerical integrations (which are often the most difficult part of higher-order calculations in QED) converge considerably faster. Typically, where comparisons could be made, the numerical integration time was between 2 and 5 times faster than the standard Feynman parameter method. This gain more than offsets the extra effort required to perform the infinite-momentum-frame algebra before integration.

These successes encouraged us to try some 6th-order moment calculations. The results of this investigation for the Feynman graphs shown in Fig. 17 have already been published.[24]

Meanwhile, Fig. 17(a) has been computed analytically by Levine and Roskies.[25] Its value is [in units of $(\alpha/\pi)^3$]

$$\frac{g-2}{2}=\frac{733}{1728}+\frac{59\pi^2}{648}+\frac{7}{18}\zeta(3)=1.790\,277\,8\,,$$

to be compared with our estimate

$$1.777\pm 0.013\,.$$

V. COVARIANT APPROACH AT $P=\infty$

Field theories at infinite momentum have been studied from a different point of view. Kogut and Soper[6] argued that the limit $P\to\infty$ is a reformulation of the theory in which the equal-time surface (in the regular frame) is replaced by a lightlike surface, i.e., $v=c$. Making the transformation

$$\tau=\frac{t+z}{\sqrt{2}}\,,$$

$$z'=\frac{t-z}{\sqrt{2}}\,,$$

they quantized the theory at equal τ. When passing from the Lagrangian to this Hamiltonian in this approach they found that the interaction Hamiltonian contained in addition to the usual piece a seagull term with the structure

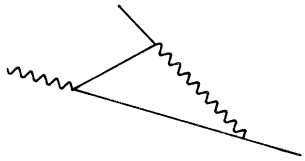

FIG. 16. Vertex insertion for the Feynman "corner" graph of Fig. 15.

$$e^2\delta(\tau-\tau')\bar{\psi}\psi A_\mu A_\nu\,,$$

that is, an instantaneous interaction involving two fermions and two photons. They then formulated TOPTh for this theory and reproduced the rules we have been discussing. In this approach the limit $P\to\infty$ never appears; it has already been taken. The question of whether this theory is equivalent to the usual one is the question of whether the $P\to\infty$ limit is justified. Their approach was formulated in the Coulomb gauge, which is difficult to renormalize. Our results indicate that their rules are correct for renormalized amplitudes, and we have shown how to implement the renormalization procedure. A more covariant approach was developed by Chang, Root, and Yan.[9,26] Starting with Schwinger's action principle, they "derived" the equal-τ commutation relations which Kogut and Soper had guessed. They found that the Feynman propagator was identical to the usual one for spin zero, but differed for spin $\frac{1}{2}$. But they were able to show that the extra term in the spin-$\frac{1}{2}$ propagator exactly canceled the terms arising from the seagull term in the interaction Hamiltonian, so that their theory formally agreed with the usual one for renormalized amplitudes. Their expressions for the renormalization constants differed from the usual Feynman ones.

These results are easily understandable in terms of ours. Because the Feynman propagator only involves free fields, and because all free particles have $x>0$, the fermion propagator does not include fermions with negative x. These must be contained

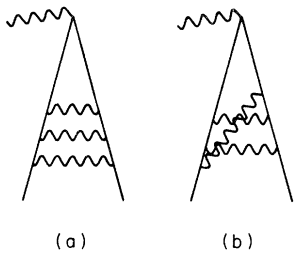

FIG. 17. Feynman graph contributions to the sixth-order magnetic moment computed using time-ordered perturbation-theory techniques.

in the effective interaction Hamiltonian, and they are exactly the seagull term. We have seen that fermions of negative x extend only over one time interval, so that no other interaction can occur between its vertices. One can then effectively assume that its vertices are simultaneous. Formally one can also see this by noticing that the energy denominator aasociated with a state containing a particle of negative x is independent of the external energy, so that its Fourier transform is a δ function in time. Moreover, the seagull term, a contracted z graph, clearly involves two external fermions and two photons.

In a theory of scalar particles with no derivative coupling, our rules showed that at $P\to\infty$ there were no particles of negative x. Thus, the free propagator should agree with the Feynman result.

We can also understand why, for example, their expression for δm_e does not agree with ours. As a field theory, it was natural to interpret the seagull term as a normal-ordered expression. But that means that it will not contribute to δm_e since its expectation value must be taken between states which have no photons. But we have seen that the seagull does contribute to the usual Feynman answer for δm_e, although its omission does not alter any renormalized amplitude. Bouchiat *et al.*[8] have shown that if one does not normal-order the seagull, the Feynman expression for δm_e is obtained.

VI. CONCLUSIONS

We have demonstrated that TOPTh at infinite momentum is a viable practical calculational technique for higher-order processes in QED. We have shown how to implement the renormalization procedure in a manner which closely parallels the usual method, and have demonstrated that for renormalized amplitudes the limit $P\to\infty$ may be taken before performing the phase-space integrations, although this is not true in evaluating the renormalization constants themselves. Many of the concepts of the Feynman approach, such as off-mass-shell behavior, factorized vertices and self-energy parts, and trace techniques, have a natural place in TOPTh$_\infty$.

We have shown that our rules are equivalent to those obtained from quantizing on the light cone, but the study of the limit $P\to\infty$ allows us to extend that analysis to include a consistent renormalization program. Moreover, the discrepancy between the value of the renormalization constants evaluated in the light-cone method and in the usual Feynman method is resolved. Our analysis puts field-theoretic parton calculations on a rigorous basis, provided that a covariant regularization procedure is used.

Some of the advantages of TOPTh at infinite momentum are:

(1) There is manifest unitarity, i.e., intermediate states have a definite number of on-mass-shell particles. This is sometimes more useful than manifest covariance. This is particularly true for bound-state problems where one is dealing with wave functions.

(2) The integrations over $\vec{k}^2$ and x in renormalized amplitudes are well behaved at the end points and are suitable for numerical evaluation.

(3) Because of the close resemblance of this formulation with nonrelativistic theory, it is hoped that this approach will lead to a deeper understanding of field theory and to new approximation schemes for both QED and hadron physics. A procedure for calculating the bound-state energies of positronium has already been developed by Feldman *et al.*[27] This method has been used to extend the impulse approximation to relativistic problems,[4] to calculate high-energy Compton scattering[28] and rearrangement collisions for relativistic systems.[29]

ACKNOWLEDGMENTS

It is a pleasure to acknowledge conversations with A. Casher, R. Goble, K. Johnson, D. Kershaw, M. Levine, J. Gunion, R. Blankenbecler, J. Bjorken, S. Drell, and T.-M. Yan.

One of us (R. R.) wishes to thank Yale University for the award of a Junior Faculty Fellowship for the academic year 1971–1972, thank S. Drell for the hospitality of the theoretical physics group at SLAC, where most of this work was performed, and thank Y. Ne'eman for the hospitality of the physics department at Tel-Aviv University.

APPENDIX: THE CONNECTION BETWEEN FEYNMAN AND INFINITE-MOMENTUM RULES

In this appendix we give a simple connection between the Feynman rules and TOPTh in the infinite-momentum frame for some low-order graphs. This discussion extends the work of Chang and Ma[5] and Schmidt.[30]

Consider, as a first example, the calculation of the lowest QED vertex labeled as in Fig. 10. We retain the kinematics of Sec. IV. The Feynman rules give

$$M_\nu = \int \frac{d^4k/i}{(2\pi)^4} \frac{\gamma^\mu(\not p_1+m)\gamma_\nu(\not p_2+m)\gamma_\mu}{(p_1^2-m^2+i\epsilon)(p_2^2-m^2+i\epsilon)(k^2-\lambda^2+i\epsilon)}. \tag{A1}$$

We parametrize the four-momenta as follows ($\vec{q}^2 = -q^2$):

$$q = (0, \vec{q}, 0),$$

$$p = \left(P + \frac{m^2 + \frac{1}{4}\vec{q}^2}{4P}, \vec{0}, P - \frac{m^2 + \frac{1}{4}\vec{q}^2}{4P}\right), \tag{A2}$$

$$k = \left(xP + \frac{k^2 + \vec{k}^2}{4xP}, \vec{k}, xP - \frac{k^2 + \vec{k}^2}{4xP}\right).$$

Notice that the mass-shell conditions for $p \pm \frac{1}{2}q$, q, and k are satisfied independent of the value of P. Thus P is an arbitrary parameter of the frame choice; $y = \ln(2P/m)$ is the rapidity of the incident electron. Of course, in the frame where $P \to \infty$, the quantity $x \equiv (k_0 + k_3)/2P$ is the fractional longitudinal momentum carried by the photon.

The four degrees of freedom of k^2 are replaced by x, $\vec{k}$, and k^2:

$$d^4k = d^2k \frac{dx}{2|x|} dk^2. \tag{A3}$$

Assuming uniform convergence, the k^2 integration may be performed immediately from the pole structure of the integrand of (A1).

$$\begin{aligned} p_1^2 - m^2 + i\epsilon &= (p + \tfrac{1}{2}q - k)^2 - m^2 + i\epsilon \\ &= (1-x)\left[m^2 + \tfrac{1}{4}\vec{q}^2 - \frac{(\vec{k})^2 + k^2}{x} - \frac{(\vec{k} - \frac{1}{2}\vec{q})^2 + m^2}{1-x}\right] + i\epsilon, \\ p_2^2 - m^2 + i\epsilon &= (p - \tfrac{1}{2}q - k)^2 - m^2 + i\epsilon \\ &= (1-x)\left[m^2 + \tfrac{1}{4}\vec{q}^2 - \frac{(\vec{k})^2 + k^2}{x} - \frac{(\vec{k} + \frac{1}{2}\vec{q})^2 + m^2}{1-x}\right] + i\epsilon. \end{aligned} \tag{A4}$$

The k^2 integration clearly is zero unless $0 \leq x \leq 1$. Closing the contour below, we pick up the $k^2 = \lambda^2 - i\epsilon$ pole and obtain

$$M_\nu = -\int d^2k \int_0^1 \frac{dx}{2x(1-x)^2} \frac{\gamma^\mu (\not{p}_1 + m)\gamma_\nu (\not{p}_2 + m)\gamma_\mu |_{k^2 = \lambda^2}}{\left[m^2 - \frac{(\vec{k} + \frac{1}{2}x\vec{q})^2 + \lambda^2}{x} - \frac{(\vec{k} + \frac{1}{2}x\vec{q})^2 + m^2}{1-x}\right]\left[m^2 - \frac{(\vec{k} - \frac{1}{2}x\vec{q})^2 + \lambda^2}{x} - \frac{(\vec{k} - \frac{1}{2}x\vec{q})^2 + m^2}{1-x}\right]}, \tag{A5}$$

which is exactly the infinite-momentum TOPTh result. Notice that p_1^μ and p_2^μ in the numerator are computed from energy conservation using the on-mass-shell calculation for the photon

$$p_1 \to (p - \tfrac{1}{2}q) - k|_{k^2 = \lambda^2} = \left((1-x)P + \frac{m^2 + \frac{1}{4}\vec{q}^2}{4P} - \frac{\lambda^2 + \vec{k}^2}{4xP}, -\vec{k} - \tfrac{1}{2}\vec{q}, (1-x)P - \frac{m^2 + \frac{1}{4}\vec{q}^2}{4P} + \frac{\lambda^2 + \vec{k}^2}{4xP}\right). \tag{A6}$$

This coincides with the rule for automatic z-graph inclusion given in Sec. II. Equation (A5) is valid for any component of M_ν, assuming regularization in the photon mass.

Let us also consider a two-loop example, the crossed-graph contribution to the electron vertex (see Fig. 15 II). We again parametrize the loop momentum as in Eq. (A2) with

$$k_{(i)}^\mu = \left(x_i P + \frac{k_i^2 + \vec{k}^2}{4x_i P}, \vec{k}_i, x_i P - \frac{k_i^2 + \vec{k}^2}{4x_i P}\right). \tag{A7}$$

The poles in k_i^2 derive from the photon propagators and

$$\begin{aligned} (p - \tfrac{1}{2}q - k_1)^2 - m^2 + i\epsilon &\sim -(1-x_1)\frac{k_1^2}{x_1} + i\epsilon + \cdots, \\ (p + \tfrac{1}{2}q - k_2)^2 - m^2 + i\epsilon &\sim -(1-x_2)\frac{k_2^2}{x_2} + i\epsilon + \cdots, \\ (p \pm \tfrac{1}{2}q - k_1 - k_2)^2 - m^2 + i\epsilon &\sim -(1-x_1-x_2)\left(\frac{k_1^2}{x_1} + \frac{k_2^2}{x_2}\right) + i\epsilon \cdots. \end{aligned} \tag{A8}$$

For $1-x_1-x_2>0$, we close the contours below, pick up contributions from $k_1^2=\lambda^2-i\epsilon$, $k_2^2=\lambda^2-i\epsilon$, and obtain a result identical to that of the infinite-momentum frame for Fig. 15 II(a). The lepton energies are obtained from energy conservation from the initial-state particles and the on-shell photons. However, for $1-x_1-x_2<0$, we close the k_1^2 and k_2^2 contours above, and pick up contributions from

$$(p+\tfrac{1}{2}q-k_2)^2=m^2-i\epsilon \quad \text{and} \quad (p-\tfrac{1}{2}q-k_1)^2=m^2-i\epsilon\,, \tag{A9}$$

and obtain the infinite-momentum result for Fig. 15 II(b). In this case the energy of the lepton lines $p+\frac{1}{2}q-k_2$ and $p-\frac{1}{2}q-k_1$ (which cross two time intervals) is obtained from the on-shell condition. For the other lepton lines, we use energy conservation between the initial and intermediate states,

$$k_1+k_2-p+\tfrac{1}{2}q=q+(p-\tfrac{1}{2}q)-(p-\tfrac{1}{2}q-k_1)-(p+\tfrac{1}{2}q-k_2) \tag{A10}$$

to determine the correct energy values. These results again agree with the automatic z-graph rule given in Sec. II.

It is of course obvious from this explicitly covariant approach that the same basic Dirac algebra or trace occurs independent of the time ordering, and it is identical to the Feynman result.

One important caution in carrying out this procedure is that the resulting $d^2k\,dx$ integration must be finite after the k^2 integration is performed; otherwise the lack of uniform convergence can be reflected by extra δ-function contributions, which reflect surviving contributions from nonforward graphs in the $P\to\infty$ TOPTh calculations.

As an example of the occurrence of an essential $\delta(x)$ contribution, let us return to the δm calculation of Sec. III F. The Feynman result is

$$\bar{u}u\,\delta m=\frac{e^2}{(2\pi)^4}\int\frac{d^4k}{i}\int\rho(\lambda^2)d\lambda^2\,\frac{\bar{u}(p)\gamma_\mu(\not{p}-\not{k}+m)\gamma^\mu u(p)}{(k^2-\lambda^2+i\epsilon)[(p-k)^2-m^2+i\epsilon]} \tag{A11}$$

or

$$m\,\delta m=\frac{e^2}{(2\pi)^4}\int d^2k\int\frac{dx}{2|x|}\int\frac{dk^2}{i}\int\frac{\rho(\lambda^2)d\lambda^2(2m^2+2p\cdot k)}{(k^2-\lambda^2+i\epsilon)[(p-k)^2-m^2+i\epsilon]}\,. \tag{A12}$$

Here we covariantly regularize in the photon mass by setting the zeroth and first moments of the spectral function $\rho(\lambda^2)$ to zero. As always the λ^2 integration is to be performed first.

The numerator can be written in the form

$$4m^2-2p\cdot(p-k)=3m^2+xm^2-\frac{\vec{k}^2+m^2}{1-x}-\frac{(p-k)^2-m^2}{1-x}\,. \tag{A13}$$

The first three terms correspond to δm_a of Sec. III, and gives Eq. (3.40) after the k^2 integration is performed. For the last term we note the distribution identity[31]

$$\frac{1}{2|x|}\int\frac{dk^2}{i}\int\frac{\rho(\lambda^2)d\lambda^2}{k^2-\lambda^2-i\epsilon}=-\tfrac{1}{2}\pi\,\delta(x)\int\rho(\lambda^2)d\lambda^2\ln(\vec{k}^2+\lambda^2)\,. \tag{A14}$$

This follows from the fact that the left-hand side of (A14) vanishes for $x\neq0$, and

$$\int\frac{d^4k}{i}\int\frac{\rho(\lambda^2)d\lambda^2}{k^2-\lambda^2+i\epsilon}=\frac{-\pi}{2}\int d^2k\int\rho(\lambda^2)d\lambda^2\ln(\vec{k}^2+\lambda^2)\,, \tag{A15}$$

which is the usual result obtained from doing the k_0 and k_3 integrations.

Thus the origin of the δm_b term Eq. (3.41), which corresponds to the singular $x\sim0$ contribution of the backward graph in the $P\to\infty$ TOPTh calculation, is the singular nature of the transformation (A3) in the k^2 integration method. Note that the explicit occurrence of the δm_b contribution can be formally avoided if one uses (the unconventional) regularization in both the internal photon and lepton masses.[31]

The extra δ-function terms can always be avoided if covariant regularization of the photon and lepton propagators is assumed, and thus never occur in our QED calculations of regularized or renor-

malized amplitudes. In the vacuum-polarization calculation, regularization in the mass of the loop fermion must be used.. In the vertex calculations, photon regularization is sufficient.

Unfortunately, this prescription of performing the k^2 integral does not always generate the TOPTh$_\infty$ integrands. This is perhaps most easily seen in tree graphs, which require no integrations. One can easily see that the Feynman amplitude is then a sum of different TOPTh$_\infty$ graphs, and no simple operation on individual propagators can reproduce the separate time-ordered integrands, because the number of surviving time orders is not always of the form (constant)^n, where n is the number of internal propagators.[32]

---

*Work supported by the U. S. Atomic Energy Commission.

†Present address: University of Pittsburgh, Pittsburgh, Pennsylvania 15260.

‡Supported in part by the U. S. Atomic Energy Commission under Contract AT(11-1)-3075.

§Present address: University of Buenos Aires, Argentina. Address after August 1: University of Illinois, Urbana, Illinois.

[1]S. Weinberg, Phys. Rev. 150, 1313 (1966). See also L. Susskind and G. Frye, *ibid.* 165, 1535 (1968); K. Bardakci and M. B. Halpern, *ibid.* 176, 1686 (1968).

[2]S. Fubini and G. Furlan, Physics 1, 229 (1965); J. D. Bjorken, Phys. Rev. 179, 1547 (1969); R. Dashen and M. Gell-Mann, Phys. Rev. Lett. 17, 340 (1966).

[3]J. D. Bjorken and E. A. Paschos, Phys. Rev. 185, 1975 (1969); R. P. Feynman, see, e.g., *High Energy Collisions,* edited by C. N. Yang *et al.* (Gordon and Breach, New York, 1969), p. 237.

[4]S. D. Drell, D. J. Levy, and T.-M. Yan, Phys. Rev. Lett. 22, 744 (1969); Phys. Rev. 187, 2159 (1969); Phys. Rev. D 1, 1035 (1970); 1, 1617 (1970); S. D. Drell and T.-M. Yan, *ibid.* 1, 2402 (1970); Phys. Rev. Lett. 24, 181 (1970).

[5]S.-J. Chang and S. K. Ma, Phys. Rev. 180, 1506 (1969); 188, 2385 (1969). Some lower-order infinite-momentum calculations were also studied in this reference and in Ref. 6, below.

[6]J. B. Kogut and D. E. Soper, Phys. Rev. D 1, 2901 (1970); J. D. Bjorken, J. B. Kogut, and D. E. Soper, *ibid.* 3, 1382 (1971). The light-cone quantization has been formulated independently by R. A. Neville and F. Rohrlich, Phys. Rev. D 3, 1692 (1971); Nuovo Cimento 1A, 625 (1972).

[7]R. Barbieri, J. A. Mignaco, and E. Remiddi, Nuovo Cimento 11A, 824 (1972); 11A, 865 (1972).

[8]C. Bouchiat, P. Fayet, and N. Sourlas, Nuovo Cimento Lett. 4, 9 (1972).

[9]S.-J. Chang, R. G. Root, and T.-M. Yan, Phys. Rev. D 7, 1133 (1973); S.-J. Chang and T.-M. Yan, *ibid.* 7, 1147 (1973), and University of Illinois reports; T.-M. Yan, Phys. Rev. D 7, 1760 (1973); 7, 1780 (1973); J. H. Ten Eyck and F. Rohrlich, Phys. Rev. D (to be published).

[10]The sign convention is a consequence of the anticommutation property of the fermion field and guarantees Fermi statistics.

[11]See the third paper of Ref. 4.

[12]See Sec. IV.

[13]The expression δm_a defined in (3.40) is still not well defined, and needs a further regularization. This can be done by writing

$$\delta m_a = \frac{e^2}{16\pi^3 m}\int d^2k \int_0^1 \frac{dx}{1-x}\int_0^\infty d\lambda\,\rho(\lambda^2) \times \frac{m^2(2-2x-x^2)-\vec{k}^2}{\lambda^2(1-x)+\vec{k}^2+m^2x^2},$$

where $\int\rho(\lambda^2)d\lambda = 0$ and $\int\lambda^2\rho(\lambda^2)d\lambda = 0$. For ease of interpretation we retain the form written in the text.

[14]It is possibly more convenient for radiative correction calculations to use a cutoff $s_\gamma = \vec{k}_\gamma^{\,2}/x_\gamma > s_{\min}$, since this can be readily matched to the real photon phase-space integrations in the $P\to\infty$ frame.

[15]S. Weinberg, Phys. Rev. 118, 838 (1960).

[16]Recall that $V = 2B_i + B_e = F_i + \frac{1}{2}F_e$. We also denote F as the number of charged particles for the spin-zero QED case.

[17]C. M. Sommerfield, Phys. Rev. 107, 328 (1957); Ann. Phys. (N.Y.) 5, 26 (1958); A. Petermann, Helv. Phys. Acta 30, 407 (1957); Nucl. Phys. 3, 689 (1957).

[18]D. Foerster, University of Sussex thesis, 1973 (unpublished). Foerster's derivation of the lowest-order anomalous moment $\alpha/2\pi$ is particularly instructive. If the electron interacts with a magnetic field (transverse photon polarization), then one finds that the contribution of Fig. 2(a) without the z-graph modification is negative (but logarithmic divergent) in agreement with Welton's classical argument [T. Welton, Phys. Rev. 74, 1157 (1948)]. The surviving z-graph contributions of Fig. 2(a) (and its mirror graph) are positive, canceling the divergent term, and leaving the finite $\alpha/2\pi$ remainder. Note that the z-graph piece contains the Thomson-limit part of the Compton amplitude for the sidewise dispersion calculation of S. Drell and H. Pagels, Phys. Rev. 140, B397 (1965). The remaining diagrams in Fig. 2 vanish in the infinite-momentum frame.

[19]A. C. Hearn, Stanford University Report No. ITP-247 (unpublished); and in *Interactive Systems for Experimental Applied Mathematics,* edited by M. Klerer and J. Reinfields (Academic, New York, 1968).

[20]See J. Aldins, S. Brodsky, A. Dufner, and T. Kinoshita, Phys. Rev. D 1, 2378 (1970); A. Dufner, in *Proceedings of the Colloquium on Computational Methods in Theoretical Physics* (Marseille, 1970); and B. Lautrup, in *Proceedings of the Second Colloquium on Computational Methods in Theoretical Physics* (Marseille, 1971).

[21]In general a graph with n loops requires a maximum of $(3n-1)$ integrations, as opposed to the Feynman parameter approach requiring $(3n-2)$. Symmetries of graphs reduce the dimensionalities by the same number in both approaches.

[22]For numerical integrations we used the transformation $\vec{k}_i^2 = x_i^2(1/z_i - 1)$, $0 \le z_i \le z_i \le 1$. This makes the range of all variables finite. This particular transformation also trivializes the second-order moment calculation and we hoped it would smooth the higher-order integrals.
[23]See for example, S. J. Brodsky and J. D. Sullivan, Phys. Rev. 156, 1644 (1967).
[24]S. Brodsky and R. Roskies, Phys. Lett. 41B, 517 (1972).
[25]M. Levine and R. Roskies, Phys. Rev. Lett. 30, 772 (1973).
[26]A similar result has been obtained independently by T.-M. Yan, Phys. Rev. D 7, 1781 (1973).
[27]G. Feldman, T. Fulton, and J. Townsend, Ann. Phys. (N.Y.) (to be published).
[28]S. Brodsky, F. Close, and J. Gunion, Phys. Rev. D 5, 1384 (1972).
[29]J. Gunion, S. Brodsky, and R. Blankenbecler, Phys. Rev. D 6, 2652 (1973); Phys. Lett. 39B, 649 (1972).
[30]M. Schmidt, Phys. Rev. D (to be published); see also S. Brodsky, F. Close, and J. Gunion, Phys. Rev. D 8, 3678 (1973).
[31]We wish to thank J. Kogut and D. Soper for a discussion on this point.
[32]A general discussion of the connection between the TOPTH_∞ and Feynman rules will be presented elsewhere.